Nanofabrication

DOI: 10.1002/anie.200701496

Fluorocarbon Resist for High-Speed Scanning Probe Lithography**

*Marco Rolandi, Itai Suez, Andreas Scholl, and Jean M. J. Fréchet**

In the past two decades, scanning probe lithography (SPL) has developed as an extremely versatile nanofabrication tool[1] and a powerful technique for exploring localized surface chemistry.[2] A variety of surfaces have been patterned including silicon,[3] metals,[4,5] and rare-earth metal oxide blends.[6,7] Organic substrates have been modified as resist layers for etching[8,9] and as templates for directed assembly.[10,11] Organic molecules have also served as "inks" for the AFM probe employed as the nib of a dip pen.[12] Recently, exposure of common organic solvents to the electric field generated by a biased AFM tip has afforded etch-resistant features as narrow as 4 nm.[13–16] Despite an abundance of techniques, the scope of SPL is still limited by low throughput. Significant room for improvement lies in patterning in parallel[17] or in increasing tip speed. The tip speed is nm s^{-1} for dip pen nanolithography,[12] μm s^{-1} for high field patterning,[13,14] and mm s^{-1} for the fastest siloxane-based positive tone resists.[18,19]

Herein, we present a novel SPL that reliably patterns large areas with etch-resistant sub-50 nm features at velocities in the cm s^{-1} range. In brief, a biased AFM tip traces desired shapes on the sample while immersed in perfluorooctane (PF8; Figure 1a). The electric field (approximately 10^9 V m^{-1}) in the small gap between the tip and the surface decomposes the solvent into radicals that react to deposit a fluorinated amorphous carbon film (Figure 1b).[20] In this way, lines as narrow as (27 ± 2) nm (full width at half maximum) and 0.7-nm tall were fabricated at rates of 1 cm s^{-1} (Figure 1c).

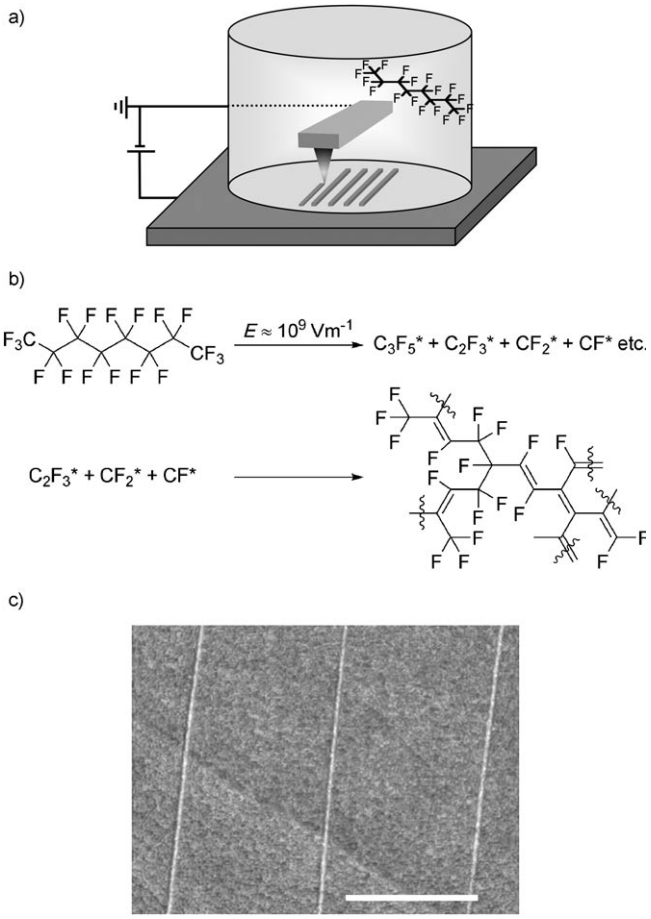

Figure 1. a) Illustration of the setup for SPL in PF8, both the AFM probe and the sample surface are immersed in the solvent. Lithography is performed by translating the grounded tip across desired locations on the biased sample. b) Mechanism for formation of fluorinated amorphous carbon film: PF8 decomposes into many species such as C_2F_3, CF_2, and CF radicals that recombine to form amorphous fluorocarbon.[20] c) Tapping-mode AFM image of lines written in the contact mode at +12 V bias on the sample and with a tip speed = 1 cm s^{-1}. Scale bar = 1 μm. The image was illuminated from the right-hand side for contrast enhancement.

The patterns demonstrated excellent resistance in fluorinated dry etchants (Figure 2); negative tone features that were 50-nm wide were readily transferred 20 nm into the substrate by using SF_6 gas plasma. Lithography for the entire area shown in Figure 2a, including processing of the instructions by microscope electronics, only required 15 seconds. In the same 15 s, high-field lithography in octane would only have written a single 150-nm-long line,[16] and e-beam lithography[21] would have written at most 1/4 of the structure.

The chemical composition of the features was elucidated through the near-edge X-ray absorption fine structure

[*] Dr. M. Rolandi, Dr. I. Suez, Prof. J. M. J. Fréchet
College of Chemistry
University of California
Berkeley, CA 94720 (USA)
Fax: (+1) 510-643-3079
E-mail: frechet@berkeley.edu
Dr. A. Scholl
Advanced Light Source
Lawrence Berkeley National Laboratory
Berkeley, CA 94720 (USA)
Dr. M. Rolandi, Prof. J. M. J. Fréchet
Materials Sciences Division
Lawrence Berkeley National Laboratory
Berkeley, CA 94720 (USA)

[**] Financial support from the Director, Office of Science, Office of Basic Energy Sciences, the U.S. Department of Energy under contract number DE-AC02-05CH11231, NSF-SINAM, and SRC-DARPA is gratefully acknowledged. M.R. thanks INTEL for post-doctoral funding through the Materials Sciences Division, LBNL. The authors thank Dr. T. Mates, D. Okawa, Dr. D. Mair, Dr. S. A. Backer, Dr. S. Rajaram, and Dr. A. Doran for assistance in characterization experiments and insightful discussions.

Supporting information for this article is available on the WWW under http://www.angewandte.org or from the author.

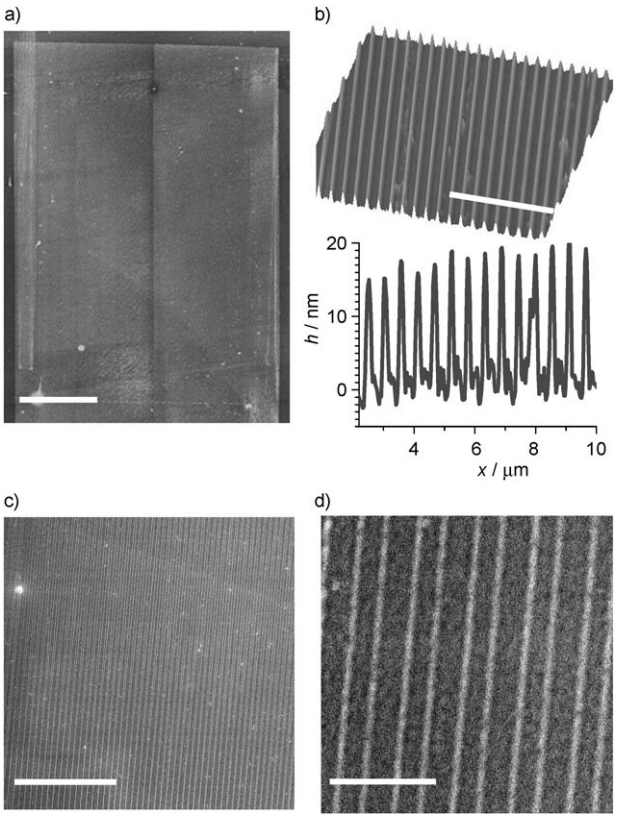

Figure 2. a) Large-scale tapping-mode AFM image of a pattern written at 12 V and 1 cm s^{-1} after 5 s dry etch in SF6. Scale bar = 25 μm. b) Zoomed-in section of the image shown in Figure 2a and the horizontal cross section; scale bar = 5 μm. c and d) Scanning electron micrographs of the same area; scale bars = 10 μm and 1.5 μm, respectively.

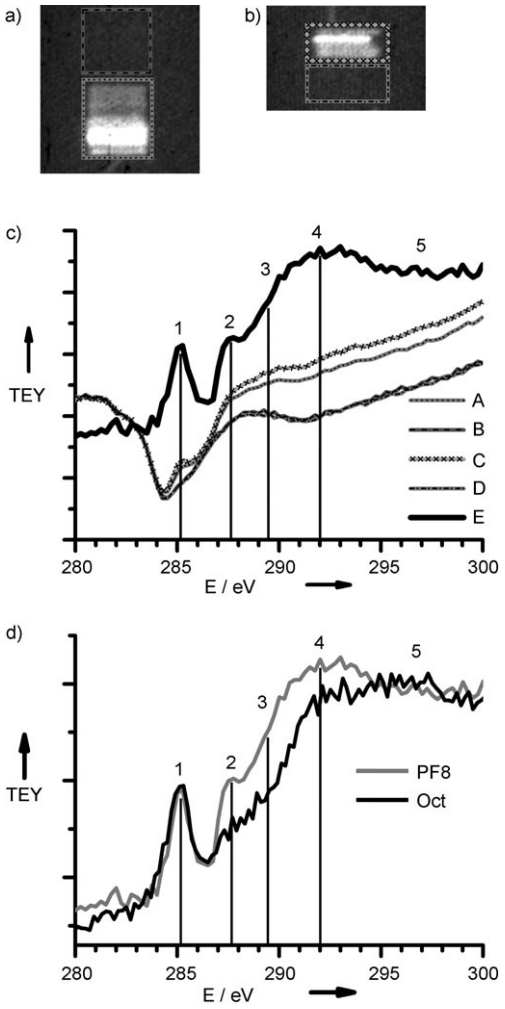

Figure 3. a and b) PEEM images of the patches made by using high-field lithography in PF8, acquired at 300 eV X-ray energy, above the C K edge. c) Local X-ray absorption spectra acquired in the patterned areas located on (A and C) and off (B and D) the patches. The spectra represent raw data and were recorded in the boxes outlined in the same color in panels (a) and (b). The black trace shows the spectrum E = (A + C)/(B + D), which displays the chemical signature of the written patch. d) Comparison of two normalized PEEM spectra acquired on a patch made with octane (black) and perfluorooctane (gray). TEY = total electron yield.

(NEXAFS) recorded by a photo emission electron microscope (PEEM). NEXAFS is based on X-rays exciting core electrons into bound empty states to probe the unoccupied molecular orbitals. To facilitate analysis, larger microscopic patches were fabricated by using SPL in PF8 (Figure 3a and Figure 3b). The colored curves in Figure 3c correspond to absorption spectra acquired by the PEEM around the C K edge on and off the patches; the black trace shows the average of the signal on the patch divided by the signal off the patch. The latter serves as an I_0 correction to compensate for the energy dependence of the X-ray flux in the beam line. Analysis of the spectra identifies the bonding network of the film. The lower energy resonance (1) at 285.3 eV corresponds to the transition of a photoelectron from the K shell of C to the π* orbital of C=C–C; the wide band (5) with an onset at approximately 290 eV is assigned to the transitions to the σ* orbitals and indicates a significant presence of sp^3 hybridized carbon. Peak (2) at 287.5 eV, which is a signature peak of C=C–F[22] is clearly absent in the spectrum acquired on a patch made with simple octane (Figure 3d). The onset of the σ* band at lower energies for the PF8 patterned sample suggests the presence of two additional peaks at 290 eV (3) and 292 eV (4). The first is assigned to the transition to the π* orbital of $C{=}CF_2$[22] and the second to the σ* orbital of C–C–F.[23] The ratio of the integrals of the σ* and π* peaks is used as an estimate of the sp^2/sp^3 content in the material.[24] In this sample, approximately 1/3 of the C has unsaturated bonds, suggesting the formation of a cross-linked network.

The contents of the patterns were confirmed by elemental depth profiling with secondary ion mass spectrometry (SIMS; Figure 4). In the image sequence from Figure 4b to Figure 4h, the brighter parts represent the fluorine content of the debris arising from the patterned area that is etched away by a high-energy Ga beam. In the first SIMS image (Figure 4b), significant fluorine is present everywhere on the sample as may be expected from solvent contamination. As the ion beam etches down, the surrounding area is cleaned while the fluorocarbon on the patches is still present, resulting in an increasing contrast (Figure 4d) until the entire structure is etched away (Figure 4h).

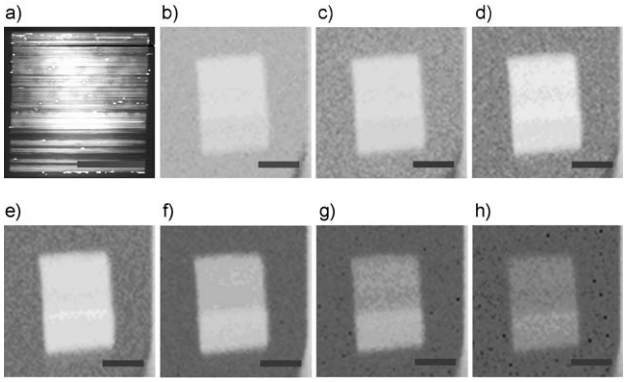

Figure 4. a) AFM image of one of the patches that was used for SIMS characterization. b–h) Sequence of images taken of the F^- (atomic weight of 19 g mol^{-1}) ion counts in accumulation intervals of 60 s. Scale bars = 10 μm.

From these analyses, we conclude that the material deposited is fluorinated amorphous carbon; this is consistent with plasma deposition with PF8 as a precursor.[25] Although the presence of fluorine in the patterns might be explained by invoking the higher strength of C–F bonds compared with C–C bonds in PF8, a comparison of bond energies for PF8 and octane does not support the dramatic difference in the deposition rate between the two.[13,14] A simple model for dielectric breakdown of solvents in high-voltage transformers[26] can also be applied to our system. Local heating in the strong field region at the sharp tip vaporizes the solvent and creates low-density regions (streamers) where discharge and formation of radicals occurs. Streamers propagate from the tip towards the sample surface, where the radicals couple and deposit as an amorphous carbonaceous film. Breakdown occurs faster in perfluorooctane because the propagation speed of negative streamers (from negative tip to positive sample) in the fluorinated solvent is two orders of magnitude higher than in octane.[26]

In conclusion, we have developed a facile high-speed SPL that can pattern nanoscopic features of fluorinated amorphous carbon at velocities of 1 cm s^{-1}. This is the fastest AFM lithography reported to date with a speed that is only limited by the piezo response. We have successfully patterned areas of 100 μm^2 in seconds and carried out negative-tone transfer in dry etch. Possible applications of nanopatterned fluorinated amorphous carbon include low *k* dielectric insulation of on-chip interconnects and patterned low energy surfaces. An advantage of this simple technique is that it can be extended to any flat conducting substrate.

Experimental Section

Si (100) substrates (Addison Engineering, B doped, $\rho = 0.02\,\Omega$ cm) were cleaned by sonication in acetone, isopropyl alcohol, water, and 15 s of oxygen plasma (SiO_2 thickness 1.8 ± 0.3 nm). Perfluorooctane (98%, Aldrich) was used as received. Lithography was performed on a Digital Instruments Multimode AFM with a fluid cell that was operated in contact mode with Sb-doped Si cantilevers Veecoprobes ($\rho = 0.02$–$0.025\,\Omega$ cm, $k = 0.2$ N m^{-1}). A bias (+6–+12 V) was applied to the sample through the Nanoscope IIIa controller. The force set point was the same as for imaging. Dry etching was implemented in a technics-c with SF_6 plasma at 194 mT, flow rate 13 sccm, and 300 W power. Scanning electron microscopy was performed with a Hitachi-S5000 operated with a 10 kV accelerating voltage and 12 μA current.

Spectromicroscopic characterization was carried out at beamline 7.3.1 (PEEM-2) of the Advanced Light Source at the Lawrence Berkeley National Laboratory. PEEM records the TEY, a measure of the X-ray absorption of the sample, with a maximum spatial resolution of approximately 50 nm. Local C K edge NEXAFS spectra were obtained with approximately 0.3 eV energy resolution from stacks of PEEM images taken at successive X-ray energies. The detector dark current was subtracted and the spectra were normalized to unity from 5 to 10 eV before the edge jump to extract chemical information that is encoded in the energy-dependent absorption of the sample. Non-energy-dependent effects caused by differences in illumination and local work function were thus removed.

SIMS was conducted at the Materials Research Laboratory of UC Santa Barbara with a Dynamic Physical Electronics 6650 Quadrupole SIMS by using a Ga liquid metal gun (LMIG) FEI model 83-2LI, which was operated at 25 kV and with a current of 350 pA. Images including F (mass 19) were collected for periods of 120 cycles, each cycle equaling 0.5 s.

Received: April 6, 2007
Published online: August 14, 2007

Keywords: electron microscopy · mass spectrometry · nanostructures · scanning probe lithography · surface chemistry

[1] J. Loos, *Adv. Mater.* **2005**, *17*, 1821–1833.
[2] R. Garcia, R. V. Martinez, J. Martinez, *Chem. Soc. Rev.* **2006**, *35*, 29–38.
[3] P. Avouris, T. Hertel, R. Martel, *Appl. Phys. Lett.* **1997**, *71*, 285–287.
[4] E. Dubois, J. L. Bubendorff, *J. Appl. Phys.* **2000**, *87*, 8148–8154.
[5] M. Rolandi, C. F. Quate, H. Dai, *Adv. Mater.* **2002**, *14*, 191–194.
[6] Y. Yanagisawa, M. Hirooka, H. Tanaka, T. Kawai, *J. Appl. Phys.* **2006**, *100*, 124316.
[7] L. Pellegrino, Y. Yanagisawa, M. Ishikawa, T. Mastumoto, H. Tanaka, T. Kawai, *Adv. Mater.* **2007**, 18, 3099–3104.
[8] G. Y. Liu, Y. L. Qian, *Acc. Chem. Res.* **2000**, *33*, 457–466.
[9] M. Rolandi, I. Suez, H. Dai, J. M. J. Fréchet, *Nano Lett.* **2004**, *4*, 889–893.
[10] R. Maoz, E. Frydman, S. R. Cohen, J. Sagiv, *Adv. Mater.* **2000**, *12*, 725–731.
[11] S. A. Backer, I. Suez, Z. Fresco, M. Rolandi, J. M. J. Fréchet, *Langmuir* **2007**, *23*, 2297–2299.
[12] D. S. Ginger, H. Zhang, C. A. Mirkin, *Angew. Chem.* **2004**, *116*, 30–46; *Angew. Chem. Int. Ed.* **2004**, *43*, 30–45.
[13] I. Suez, S. A. Backer, J. M.J Fréchet, *Nano Lett.* **2005**, *5*, 321–324.
[14] R. V. Martinez, R. Garcia, *Nano Lett.* **2005**, *5*, 1161–1164.
[15] M. Tello, R. Garcia, J.A. Martín-Gago, N. F. Martinez, M. S. Martín-González, L. Aballe, A. Baranov, L. Gregoratti, *Adv. Mater.* **2005**, *17*, 1480–1483.
[16] R. V. Martinez, N. S. Losilla, J. Martinez, Y. Huttel, R. Garcia, *Nano Lett.* **2007**, 7, 1846–1850.
[17] K. Salaita, Y. H. Wang, J. Fragala, R. A. Vega, C. Liu, C. A. Mirkin, *Angew. Chem.* **2006**, *118*, 7378–7381; *Angew. Chem. Int. Ed.* **2006**, *45*, 7220–7223.
[18] S. W. Park, H. T. Soh, C. F. Quate, S. I. Park, *Appl. Phys. Lett.* **1995**, *67*, 2415–2417.
[19] H. Sugimura, N. Nakagiri, *Nanotechnology* **1997**, *8*, A15–A18.
[20] C. P. Lungu, A. M. Lungu, Y. Sakai, H. Sugawara, M. Tabata, M. Akazawa, M. Miyamoto, *Vacuum* **2000**, *59*, 210–219.

[21] F. Frulex-Cornu, J. Penaud, E. Dubois, M. François, M. Muller, *Mater. Sci. Eng. C* **2006**, *26*, 893 – 897.
[22] Y. Ma, H. Yang, J. Guo, C. Sathe, J. Nordgren, *Appl. Phys. Lett.* **1998**, *72*, 3353 – 3355.
[23] C. I. Butoi, N. M. Mackie, L. J. Gamble, D. G. Castner, J. Barnd, A. M. Miller, E. R. Fisher, *Chem. Mater.* **2000**, *12*, 2014 – 2024.
[24] C. Ziethen, O. Schmidt, G. K. L. Marx, G. Schönhense, R. Frömter, J. Gilles, J. Kirschner, C. M. Schneider, O. Gröning, *J. Electron Spectrosc. Relat. Phenom.*.**2000**, *107*, 261 – 271.
[25] C. Biloiu, I. A. Biloiu, Y. Sakai, H. Suguwara, A. Ohta, *J. Vac. Sci. Technol. A* **2004**, *22*, 1158 – 1165.
[26] Y. Nakao, T. Yamazaki, K. Miyagi, Y. Sakai, H. Tagashira, *Electr. Eng. Jpn.* **2002**, *139*, 1 – 8.

